Hindawi
Advances in Materials Science and Engineering
Volume 2019, Article ID 9087538, 11 pages
https://doi.org/10.1155/2019/9087538

Research Article

Cost-Effective Treatment of Hemihydrate Phosphogypsum and Phosphorous Slag as Cemented Paste Backfill Material for Underground Mine

Xilong Xue,[1] **Yuxian Ke**,[2] **Qian Kang**,[1] **Qinli Zhang**,[3] **Chongchun Xiao**,[3] **Fengjian He**,[4] **and Qing Yu**[1]

[1]*School of Resources Environment and Safety Engineering, University of South China, Hengyang 421001, China*
[2]*School of Resources and Environmental Engineering, Jiangxi University of Science and Technology, Ganzhou 341000, China*
[3]*School of Resources and Safety Engineering, Central South University, Changsha 410083, China*
[4]*Changsha Design and Research Institute of Nonferrous Metallurgical Co., Ltd, Changsha 410001, China*

Correspondence should be addressed to Xilong Xue; xxl3305usc@hotmail.com and Yuxian Ke; cqdjliuyue@sina.com

Received 22 October 2018; Revised 29 November 2018; Accepted 5 December 2018; Published 3 February 2019

Academic Editor: Teresa M. Piqué

The environmental pollution caused by the discharge of phosphogypsum (PG) and phosphorous slag (PS) is a common issue for all countries. In order to fully utilize hemihydrate PG (HPG) and PS and treat goafs in mines, the HPG and PS were used as cementitious materials for cemented paste backfill (CPB). The physical and chemical properties of HPG and PS were first analyzed, and then, the characteristics of CPB were evaluated through fluidity tests, gas detection, uniaxial compressive strength (UCS) tests, bleeding tests, and scanning electron microscopy (SEM). After this, the underground environmental impact of CPB-based HPG and PS was investigated through a dynamic leachability experiment. The results show that (1) the UCS of CPB increases with the increase of the HPG content and mass fraction, and the addition of 3% quicklime can eliminate CO_2, H_2S, and SO_2 generated from the slurry of CPB-based HPG-PS; (2) the addition of 3% quicklime and 5% cement to the HPG-PS mixtures can offset the strength loss of CPB in the late curing stage; (3) the UCS of the recommended specimen reaches 1.15–3.32 MPa after curing from 7 to 28 days, with their slump values varying from 15 mm to 26 mm, and the bleeding rates between 0.87% and 1.15%, which can meet the technical requirements of mining methods; (4) the UCS of CPB is the result of the cohydration reaction of hemihydrate gypsum (HG) in HPG and active Al_2O_3 and SiO_2 in PS; and (5) the leaching indexes meet Category IV of the Chinese Groundwater Quality Standard (DZ/T 0290-2015). The results of this investigation provide a cost-efficient way for the efficient mining of phosphate resources and the comprehensive utilization of HPG and PS.

1. Introduction

Phosphogypsum (PG) is a main by-product of wet-process phosphoric acid. PG can be classified into dihydrate phosphogypsum (DPG) and hemihydrate phosphogypsum (HPG) according to different processing methods [1, 2]. DPG, the main phase of which is $CaSO_4 \cdot 2H_2O$, cannot form a solidified body without heat treatment. In contrast, HPG is mainly composed of $CaSO_4 \cdot 0.5H_2O$, which presents better self-gelling properties during $CaSO_4 \cdot 0.5H_2O$ conversion to $CaSO_4 \cdot 2H_2O$ [3]. Phosphorus slag (PS) is also a by-product of yellow phosphor production via the electric furnace method and is mainly composed of $CaSiO_3$, which contains active SiO_2 and Al_2O_3 and has weak gelling properties [4, 5]. Besides, PG and PS contain a small amount of harmful impurities such as phosphorus, fluorine, and heavy metals, which limit its comprehensive utilization [1, 6, 7].

At present, over 700 million tonnes of PG and PS have been discharged in China and approximately 8000 hectares of land have been occupied [2, 8–10]. Moreover, the total emissions of phosphorus chemical wastes are still increasing at a rate of 70–90 million tonnes per year [10, 11]. The recycling rate of PG and PS in China is less than 20%, which is mainly reused as building material [7], cementitious

material [12, 13], road base material [14], soil improvement material [15], etc. The remaining 80% is directly discharged into an open-air yard without any treatment [16, 17]. However, the P, F, and heavy metals in the PG and PS are released under the long-term repeated action of natural rainfall and sunlight, causing serious pollution to the surface water and soil [2, 18]. In addition, a large number of goafs are formed in the long-term mining of phosphate rock, which seriously threatens the surface environment and mining operation safety [19, 20]. With the rapid development of mineral processing, the problems caused by the accumulation of PG, PS, and goafs are very prominent and seriously restrict the healthy and rapid development of the phosphorus chemical industry in China.

Cemented paste backfill (CPB) is an ideal solution for the treatment of solid waste and goafs based on solid waste solidification/stabilization technology and has been widely used in the global mining industry [21–24]. In order to improve the treatment of goafs and the utilization of PG and PS, Li et al. [25] and Wang et al. [26] developed a cemented backfill technology based on DPG and cement, and this technology was successfully applied to the Kaiyang phosphate mine in Guizhou province, China. However, the consumption of cement was high, and the early uniaxial compressive strength (UCS) of the backfill body was very low. Chen et al. [27], Liu [28], and Dang et al. [29] found that the PS presented better self-gelling characteristics under the excitation of CaO and NaOH and indicated that the PS could replace the cement in CPB-based DPG and cement, which greatly reduced the cost of backfill. Additionally, Li et al. [30] and Chen et al. [31] analyzed the underground environmental impact of soluble P, F, and heavy metals released from the backfill body based on PG through static and dynamic leaching tests and found that CPB could solidify P, F, and heavy metals. These efforts not only cut down the cost of backfill but also increased the recovery rate of phosphate resources. On the other hand, the utilization proportion of DPG was been greatly improved.

Original HPG is not an ideal backfill material by itself due to its strong acidity, and the large amounts of harmful gases such as H_2S and SO_2 are generated in the filling process [32]. HPG modified by quicklime not only greatly improves the early strength of the backfill body but also eliminates the gases generated during the filling process [32]. However, the strength loss coefficient reaches 25% curing for 240 days in a humid environment [3]. The long-term stability of the strength of CPB is the key to effectively control the pressure of goafs, which means that the strength stability of CPB-based HPG must be verified in the subsequent tests. In addition, the recycling PS is also a topic of global concern, and it is necessary to develop a backfill method for the low cost and safe disposal of PS and HPG, with the aim of further expanding the application range of HPG and PS.

This article attempts to develop a new solution for CPB technology-based HPG and PS. The physical and chemical properties of raw materials were first analyzed in detail. The UCS, slump value, bleeding ratio, generated gases, and microstructural features of CPB were then evaluated. Then, the underground environmental effects of P, F, and heavy metals released from the backfill body were investigated through a dynamic leachability experiment. Finally, an engineering application of CPB-based HPG-PS is evaluated in detail.

2. Materials and Methods

2.1. Raw Materials. The main materials used in this study were HPG, PS, quicklime, and Portland cement, of which HPG and PS were, respectively taken from the waste dam of a phosphate fertilizer plant and a yellow phosphorus plant in Guizhou province, China.

(1) The HPG had a moisture content and pH value of 12% and 3.1, respectively. The main chemical components of HPG are shown in Table 1. The X-ray diffraction (XRD) of HPG is shown in Figure 1(a). The main phase of HPG was $CaSO_4 \cdot 0.5H_2O$ (hemihydrate gypsum, HG) and contained a small amount of $CaSO_4 \cdot 2H_2O$ (dihydrate gypsum, DG) and quartz (SiO_2), which presented better self-gelling properties [33]. The surface of HPG particles was coarse, and the deposits were impurities such as phosphide and fluoride [34], as shown in Figure 1(b). The particle-size distribution of HPG is shown in Figure 2(a), for which the particle size of less than 50 μm accounts for 45.34%.

(2) The PS had a moisture content and pH value of 8% and 7.8, respectively. The main chemical components of PS are shown in Table 1. According to the Chinese Standard of Technical Specification for Phosphorous Slag Powder Use in Hydraulic Concrete (DL/T 5387-2007), the basicity coefficient (M_o), the mass coefficient (K), and the activity coefficient (M_n) were 1.18, 1.24, and 0.05, respectively. Thus, PS was characterized by weak gelling activity. The particle-size distribution of PS after grinding is shown in Figure 2(b), for which the particle size of less than 50 μm accounts for 17.83%.

(3) The CaO content of quicklime powder in this paper was greater than 92%. The cement used in this study was ordinary Portland cement (P.O 32.5).

2.2. Mixing Procedures. To initially determine the range of mass fractions of backfill slurry satisfied for pipeline transportation, which were subjected to the limitations of the test materials, the auxiliary tests were first carried out. The results showed that the slurry was in the form of a paste state when the mass fractions of CPB-based HPG-PS were 66%–69%, as shown in Figures 3(a) and 3(b). Large amounts of pungent odor gases were generated during the test, and the surface of the backfill body specimen was covered with a large number of pores after being demolded, as shown in Figure 3(c). If the paste was directly filled into the goafs, these gases would cause serious pollution to the underground air. Therefore, the HPG and PS mixtures should not be directly used as backfill materials before modification.

According to the results of the auxiliary tests, 24 mix proportions were designed, as shown in Table 2.

Table 1: Main chemical compositions of HPG and PS (wt.%).

Compositions	CaO	Fe_2O_3	Al_2O_3	SO_3	SiO_2	P_2O_{5total}	P_2O_{5water}	MgO	K_2O	Na_2O	F_{total}	F_{water}	Others
HPG	30.21	0.08	0.29	44.89	1.02	0.85	0.38	0.29	0.05	0.26	0.49	0.14	21.05
PS	42.56	0.46	1.77	0.82	35.54	1.28	0.04	1.39	0.75	0.35	2.21	0.57	12.26

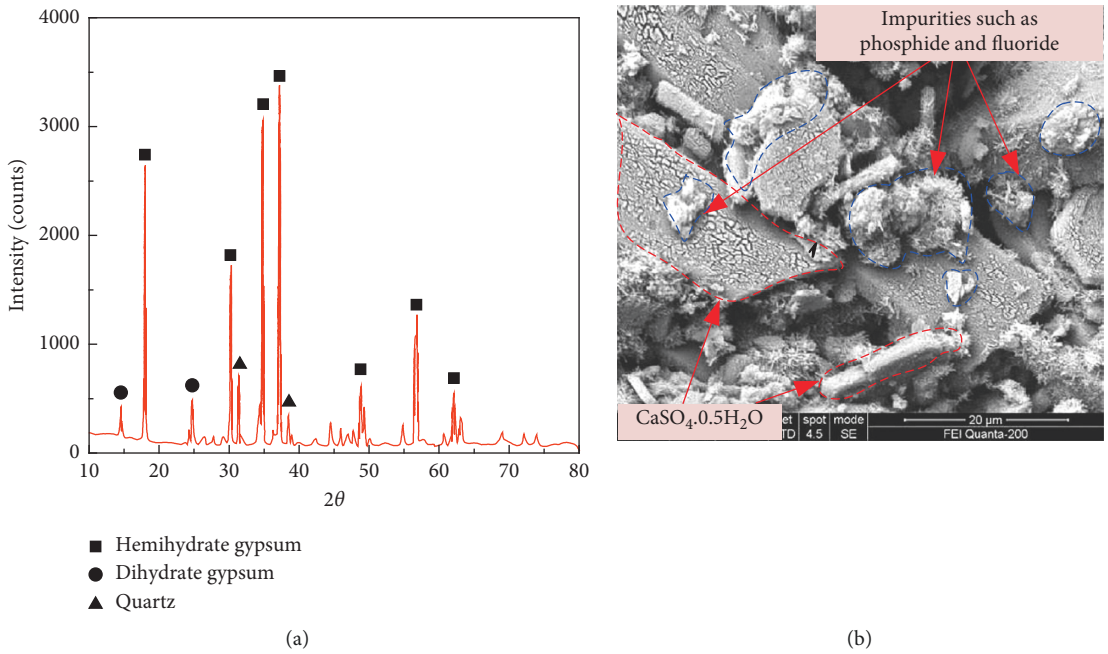

Figure 1: Results of X-ray diffraction and scanning electron microscopy (SEM) of HPG. (a) XRD image; (b) SEM image.

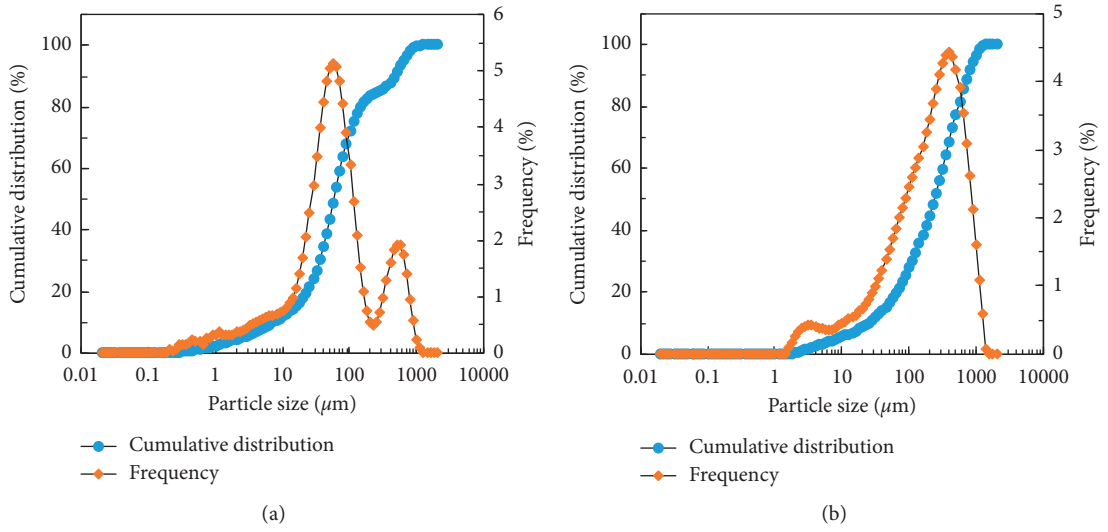

Figure 2: Curve of particle-size distribution of HPG (a) and PS (b).

Specimens S1–S15 were used to investigate the effects of the HPG/PS ratio and the quicklime content on backfill characteristics of CPB. Specimens S16–S24 were used mainly to study the strength stability of CPB over a long time period.

Based on these experiment schemes, the HPG, PS, quicklime, cement, and water were first weighed separately, and then those materials were thoroughly mixed and stirred for 5 minutes by the electric mixer. Secondly, the uniformly stirred slurry was poured into the standard triunit models with a size of 70.7 × 70.7 × 70.7 mm^3 [35], and then, the slurry was compacted with a stir bar and the mold was vibrated to keep the slurry higher than the top surface 6–8 mm of the mold. While the surface moisture was slightly dried, higher slurry is scraped from the mold to keep the surface smooth. When the slurry was completely consolidated, the mold was removed and the specimens were

(a) (b) (c)

Figure 3: Auxiliary tests process of CPB-based HPG-PS. (a) Mass fraction of 66%; (b) mass fraction of 69%; (c) backfill body with the HPG/PS ratio of 6.

Table 2: Mix proportions of HPG-PS.

No.	HPG/PS ratio	Quicklime content* (%)	Cement content* (%)	Mass fraction (%)
S1	4	0	0	66
S2	4	1	0	66
S3	4	2	0	66
S4	4	3	0	66
S5	4	4	0	66
S6	4	5	0	66
S7	6	0	0	66
S8	6	1	0	66
S9	6	2	0	66
S10	6	3	0	66
S11	6	4	0	66
S12	6	5	0	66
S13	8	3	0	66
S14	10	3	0	66
S15	14	3	0	66
S16	4	3	0	69
S17	6	3	0	69
S18	8	3	0	69
S19	10	3	0	69
S20	14	3	0	69
S21	4	3	5	69
S22	6	3	5	69
S23	8	3	5	69
S24	10	3	5	69

*The quicklime and cement were added according to the HPG quality.

numbered. Finally, the specimens were placed in a curing box with a temperature of 20°C and relative humidity of 95%.

2.3. Harmful Gas Detection. The chemical compositions of HPG and PG showed that a small amount of free ions such as S^{2-}, SO_3^{2-}, CO_3^{2-}, PO_3^{3-}, HPO_3^{2-}, and F^- might be present in the slurry, which reacted with the alkaline species in the PS to generate CO_2, H_3P, H_2S, and SO_2. The gases generated during the pulping process were detected by the method designed in a previous study [32].

2.4. Fluidity Tests. The use of a minicylinder to test the slump value is simple and accurate and can replace the ASTM standard slump test [36, 37]. It has been proven that backfill slurry with a slump value of 15–23 mm can be pumped to a stope successfully and 29–36 mm can be transported by gravity flowing [38]. To achieve better backfill application, the slump value was measured by a minicylinder with a height and diameter of 50 and 60 mm, respectively. The detailed test procedure can be found in a previous study [20].

2.5. Bleeding Tests. The bleeding rate is the main parameter that reflects the shrinkage characteristics of the backfill body [39]. In order to ensure completely roof-contacted filling in the stope, the bleeding rate should be less than 5%. In this test, the well-stirred slurry was poured into a 1000 ml cylinder to a position of 600 ml and stirred with a glass rod until the surface was free of bubbles, after which the cylinder was gently shaken and sealed. Then, the total mass of the slurry and the change of the sedimentation layer were recorded. When the sediment level ceased to change, the volume of the supernatant was read. Finally, the bleeding rate was calculated by the ratio of the quality of the bleeding to the total mass of the slurry.

2.6. UCS Tests. The UCS was tested for S1–S15 which had only been cured for 7 and 28 days, whereas S16–S24 had been cured for 3, 7, 28, 60, 120, and 180 days [40]. The UCS of specimens was tested by the WDW-2000 rigid hydraulic pressure servo machine (Ruite, Guilin, China). In order to ensure the accuracy of the test, three specimens were tested for each group.

2.7. Microstructural Analysis. After the UCS test, small specimen fragments were used for microstructure tests. Microstructural tests were carried out through commissioned tests using a scanning electron microscopy (Quanta 200, FEI, USA) in Central South University Test Center.

2.8. Dynamic Leachability Tests. To investigate the underground environmental impact of P, F, and heavy metals in CPB, the horizontal oscillating method (HJ 557-2010) (HVM) was used to investigate the dynamic leaching

behavior of original HPG, PS, and specimens cured for 28 days with the recommended parameters [41]. Then, the results were compared with Categories III and IV water quality standards of the Chinese Groundwater Quality Standard (DZ/T 0290-2015). The methods of chemical measurement were presented in a previous study [30].

3. Results and Discussion

3.1. Effect of Quicklime Content on CPB. The effects of the quicklime content on the bubbles and strength of the backfill body are shown in Figure 4. The backfill slurry was weakly acidic when no quicklime was added. With the increase of the quicklime content, the gas generated in the backfill slurry gradually decreased, and the pH value gradually increased. However, the gases were not generated when quicklime was added to 3%, and the pH value of the slurry was 7.5–7.8. Therefore, in order to reduce the cost, 3% of quicklime could be added. The generated gas was confirmed to be a mixture of H_2S, SO_2, and CO_2. Because of the presence of free ions such as SO_3^{2-}, CO_3^{2-}, and S^{2-} in the backfill slurry, these ions reacted with H^+ to form H_2S, SO_2, CO_2, and H_2O. In addition, the neutralization reaction of free SO_3^{2-}, CO_3^{2-}, S^{2-}, and F^- with $Ca(OH)_2$ in the slurry and the formation of insoluble compounds of $CaSO_4$, $Ca_3(PO_4)_2$, $Ca(H_2PO_4)_2$, and CaF_2 resulted in an increase in the pH value of the slurry. The reactions were as follows:

$$Ca^{2+} + SO_4^{2-} + 2H^+ + 2OH^- = CaSO_4\downarrow + 2H_2O \quad (1)$$

$$4Ca^{2+} + 2PO_4^{3-} + 2H_2PO_4^- + 8H^+ + 8OH^- = Ca_3(PO_4)_2\downarrow + Ca(H_2PO_4)_2\downarrow + 8H_2O \quad (2)$$

$$Ca^{2+} + 2F^- + 2H^+ + 2OH^- = CaF_2\downarrow + 2H_2O \quad (3)$$

As shown in Figure 4, when the quicklime was added from 0% to 1%, the UCS of S4 and S10 cured for 28 days was greatly decreased from 1.63 to 0.8 MPa and from 2.32 to 1.1 MPa, respectively. This indicated that HPG was sensitive to the pH value of the hydration environment, and a weakly acidic environment was beneficial to $CaSO_4 \cdot 0.5H_2O$ converting to $CaSO_4 \cdot 2H_2O$ (Equation 4). When the quicklime content increased from 1% to 3%, the UCS of S4 and S10 cured for 28 days increased from 0.8 to 1.10 MPa and from 1.02 to 1.35 MPa, respectively, and continued to increase to 5%, while the UCS decreased slightly. Therefore, the addition of 3% quicklime can achieve better strength properties for the CPB.

$$CaSO_4 \cdot 0.5H_2O + 1.5H_2O = CaSO_4 \cdot 2H_2O \quad (4)$$

3.2. Fluidity of Backfill Slurry. As shown in Figure 5(a), when the quicklime was added from 0% to 5%, the slump value of the backfill slurry did not change significantly. Therefore, the quicklime only neutralized the free acid ions in the CPB, improved the pH value of the gel system, and had no substantial effect on the fluidity of the backfill slurry.

As shown in Figure 5(b), the slump value of the slurry was between 13 and 38 mm, which decreased from 18.92%–53.57% with the slurry mass fraction increasing from 66% to 69%. When the HPG content increased from 78.13% to 90.79%, the slump value decreased from 24.32%–56.67%. This indicated that the slump value was very sensitive to mass fraction and HPG content. Due to the increase in the HPG content, water consumption increased during the $CaSO_4 \cdot 0.5H_2O$ conversion to $CaSO_4 \cdot 2H_2O$, so the free water in the slurry was reduced. In order to satisfy the requirements of pumping or gravity flowing for the backfill slurry, the slump value should be controlled between 15 and 36 mm. Therefore, HPG/PS ratios were determined to be between 6 and 10.

3.3. Bleeding of Backfill Slurry. Figure 6 presents the results of the bleeding rate tests of specimens with quicklime of 3% and different HPG/PS ratios. The bleeding rate decreased from 41.43% to 56.04% when the mass fraction increased from 66% to 69% and decreased from 35.00% to 51.22% with the HPG content increasing from 78.13% to 90.79%. Therefore, the bleeding rate of the slurry in the tests was less than 5% [39], which indicated that the shrinkage of the backfill body was small and could meet the requirements of engineering applications.

3.4. Effect of HPG Content on the Strength of Backfill Body. As shown in Figure 7, when the mass fraction of the backfill slurry with the addition of 3% quicklime increased from 66% to 69%, the UCS of the backfill body cured for 7 and 28 days increased by 33.84%–78.57% and 51.56%–74.51%, respectively. The UCS increased with the increase of the HPG content, and the growth rate continued. The main reason for this was that the increase in the HPG content led to a significant increase in the amount of $CaSO_4 \cdot 2H_2O$ converted from $CaSO_4 \cdot 0.5H_2O$ in the gelling system, which indicated that HPG played a major role in the growth of UCS. When HPG/PS ratios were less than 6, the UCS of backfill bodies cured for 7 and 28 days was 0.42–1.10 MPa and 1.02–2.25 MPa, respectively, while their UCS cured for 7 and 28 days with HPG/PS ratios of greater than 6 was 0.8–2.65 MPa and 1.35–3.88 MPa, respectively. In order to meet the requirements of the upward slicing mining method and maximize the utilization of HPG, the UCS of backfill bodies cured for 7 and 28 days should be higher than 1 MPa. Therefore, the mass fraction of CPB should be 69%, and HPG/PS ratios should be more than 6.

3.5. Long-Term Strength Characteristics of Backfill Body. As shown in Figure 8, before 28 days, the UCS of S16–S19 rapidly increased, whereas the UCS remained constant with curing from 28 to 60 days. After 60 days, the UCS began to decrease and decreased by 18.08%–35.78% until curing for 180 days, and the range decreased with the increase of the HPG content. This phenomenon basically agreed with the previous studies [3, 42], which was very unfavorable for controlling the underground pressure of the stope. In addition, when 5% Portland cement was added to the HPG-PS, the UCS of S21–S24 did not change significantly before

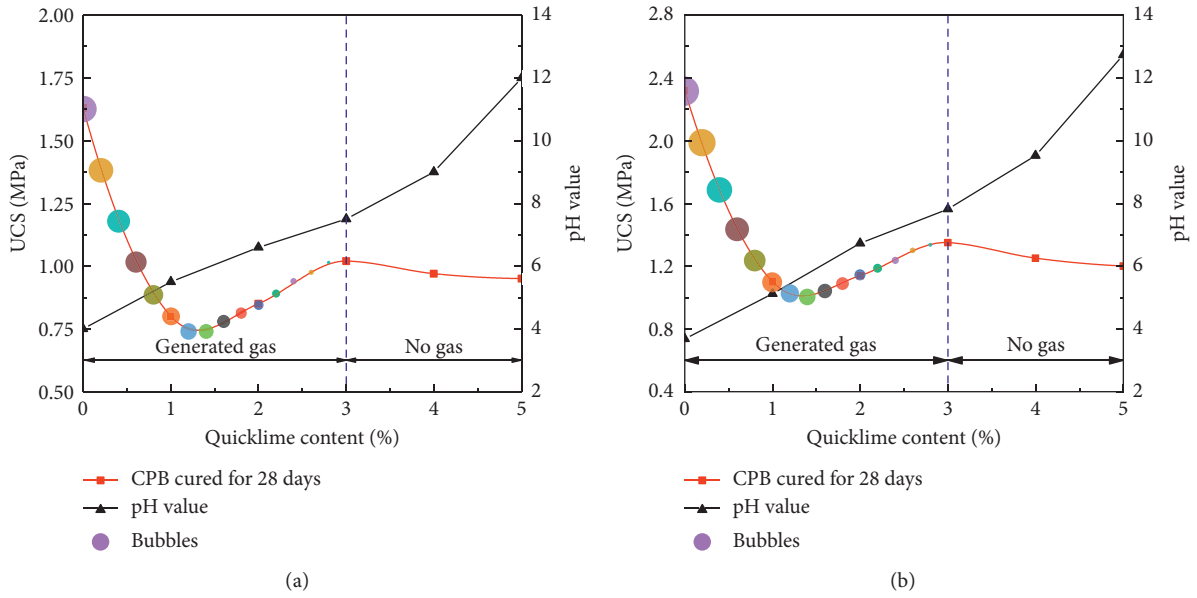

Figure 4: Effects of quicklime content on the bubbles and UCS of CPB. (a) HPG/PS ratio of 4 and mass fraction of 66%; (b) HPG/PS ratio of 6 and mass fraction of 66%.

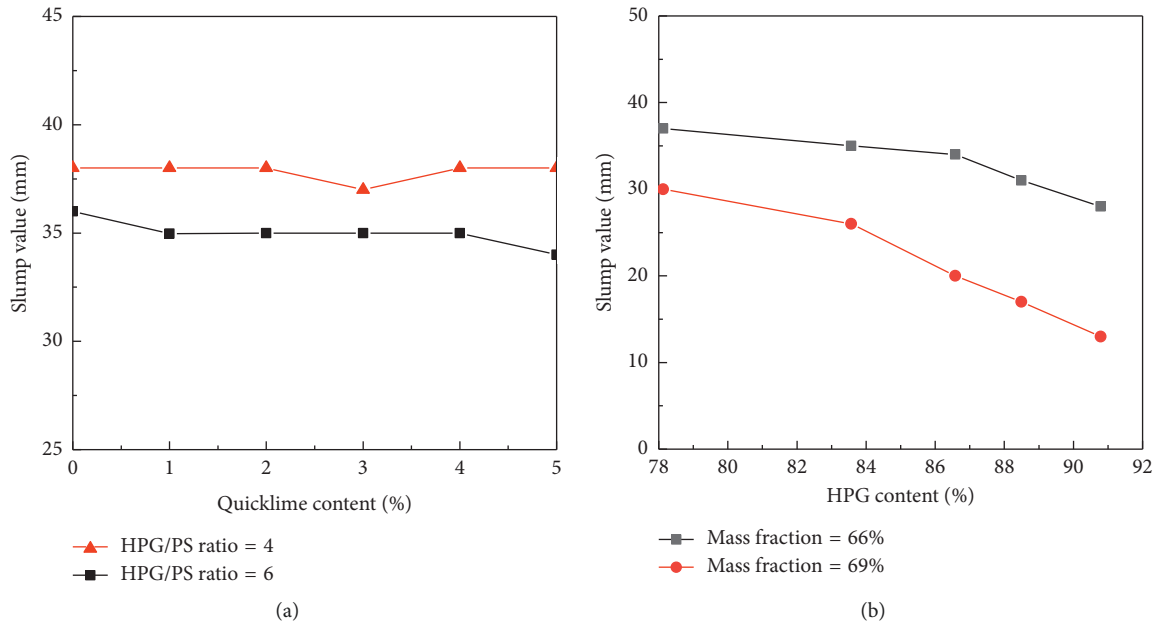

Figure 5: Effects of quicklime content and HPG content on the slump value of backfill slurry. (a) Mass fraction of 66%; (b) cement content of 3%.

28 days. After 28 days, the UCS slowly increased and maintained long-term stability, which indicated that the addition of 5% Portland cement could effectively prevent the softening of the backfill body during the later curing stage. Therefore, the recommended specimens were S21–S23, and their UCS cured for 7 and 28 days was 1.15–2.10 MPa and 2.35–3.32 MPa, respectively.

3.6. Environmental Effects. Table 3 shows the concentrations of P, F, and heavy metals in the leachate from HPG, PS, S22, and S23. The concentrations of P, F, and heavy metals in the leachate of S22 and S23 cured for 28 days were significantly lower than those of HPG and PS, and the concentration of P decreased from 3528 mg/L in the HPG to 0.38–0.62 mg/L in the backfill bodies, which indicated that the gelling system-based HPG-PS had a consolidation effect on P, F, and heavy metals [41, 43]. In addition, the concentrations of P and F in HPG leachate exceeded Category IV of DZ/T 0290-2015, and the concentrations of Fe, Mn, and Pb exceeded Category III. Moreover, the concentration of P in the leachate of S22 was between Categories III and IV of DZ/T 0290-2015, and the concentrations of the other components could meet the requirements of Category III. However, due to the large

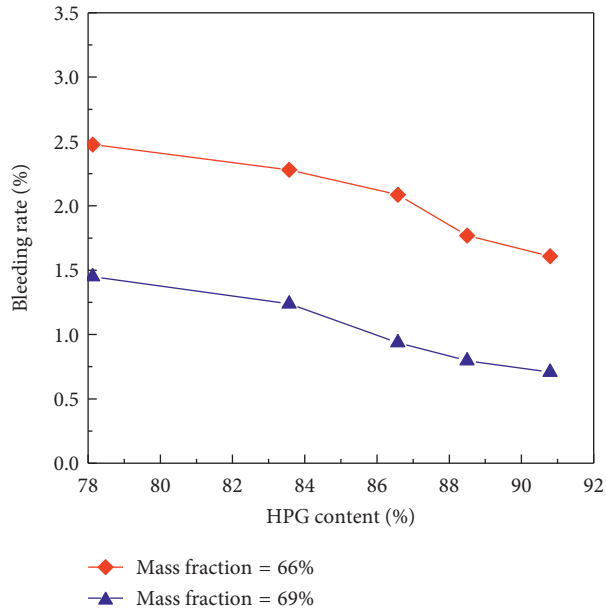

Figure 6: Effect of HPG content on the bleeding rate of backfill slurry. Cement content is 3%.

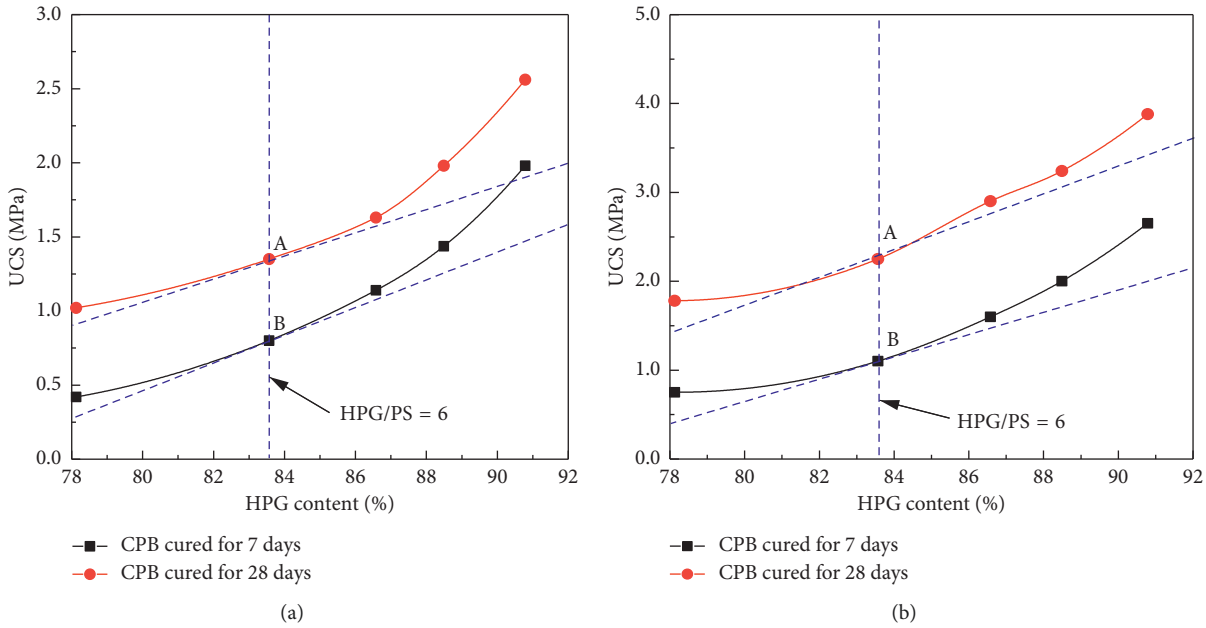

Figure 7: Effect of HPG content on the UCS of backfill body with the addition of 3% quicklime. (a) Mass fraction of 66%; (b) mass fraction of 69%.

inrush of underground water in mines and the highly developed groundwater runoff, P, F, and heavy metals were gradually diluted and transformed during the migration process, and the concentrations of the components in the practical engineering applications would be significantly reduced on the basis of the test. Therefore, the CPB-based HPG-PS hardly affected the underground environment.

3.7. Cementitious Mechanism

3.7.1. Microstructure Analysis. After 7 days, particulate substances such as $Ca_3(PO_4)_2$, $Ca(H_2PO_4)_2$, and CaF_2 [34] that were attached to the surface of the CPB material significantly reduced, and the surface gradually became thicker and smoother, as shown in Figures 9(a) and 9(c). More specifically, in some lamellar and granular $Ca(OH)_2$ crystals, a large amount of fluffy $CaSO_4 \cdot 2H_2O$ whiskers, flocculent C–S–H ($3CaO \cdot 2SiO_2 \cdot 3H_2O$) gel, and needle-like AFt (ettringite, $3CaO \cdot Al_2O_3 \cdot 3CaSO_4 \cdot 32H_2O$) are formed at the edges and between the particles. Therefore, this showed that HG in the HPG had undergone a large number of hydration, as shown in Equation (4), and partially active SiO_2 and Al_2O_3 in the PS had also undergone hydration, as shown in the following equations:

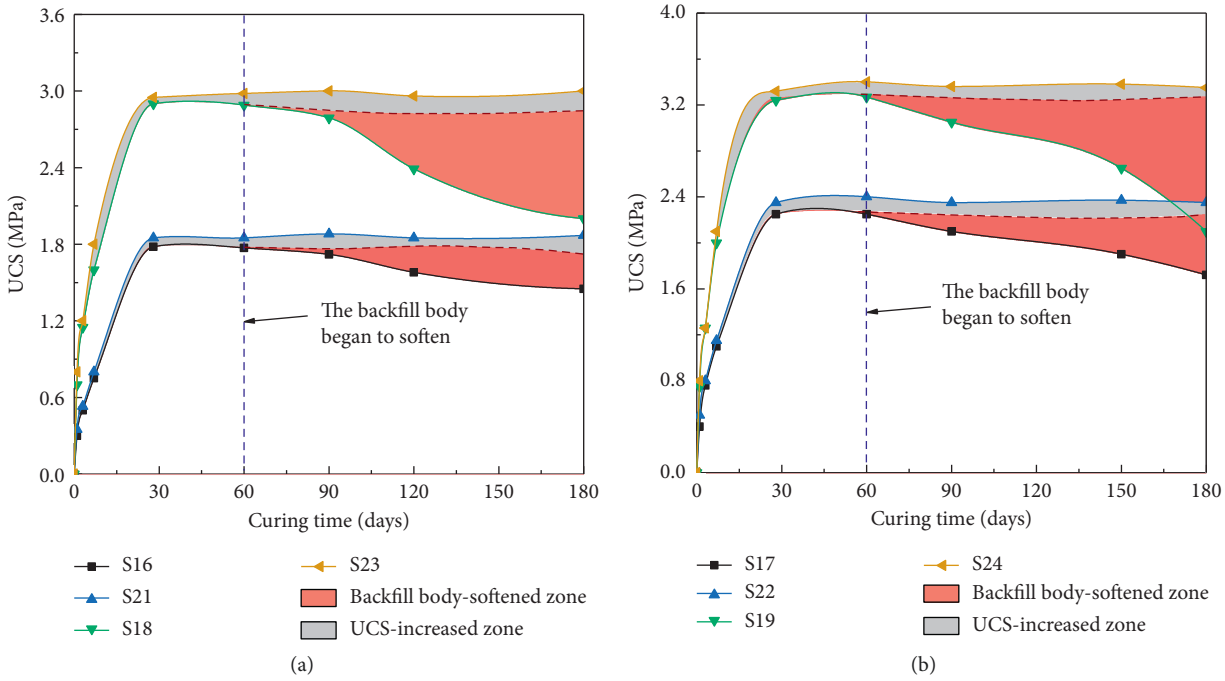

Figure 8: Long-term strength characteristics of the backfill bodies.

Table 3: Leaching elements in the HPG, PS, and backfill bodies by HVM.

Specimens	Elements (mg/L)							
	P	F	Fe	Mn	Cu	Zn	As	Pb
HPG	3528	5.3	1.35	1.4	0.1	0.05	<0.001	0.04
PS	18	3.2	0.92	<0.0001	0.05	0.04	0.01	0.01
S22 cured for 28 days	0.62	0.82	0.04	<0.0001	0.006	0.004	<0.001	<0.001
S23 cured for 28 days	0.38	0.67	0.05	<0.0001	0.009	0.005	<0.001	<0.001
Category III of DZ/T 0290-2015	0.5	1	0.3	0.1	1	1	0.01	0.01
Category IV of DZ/T 0290-2015	—	2	2	1.5	1.5	5	0.05	0.1

$$2(3CaO \cdot SiO_2) + 6H_2O = 3CaO \cdot 2SiO_2 \cdot 3H_2O + 3Ca(OH)_2 \quad (5)$$

$$3CaO \cdot Al_2O_3 + 3(CaSO_4 \cdot 2H_2O) + 26H_2O = 3CaO \cdot Al_2O_3 \cdot 3CaSO_4 \cdot 32H_2O \quad (6)$$

After 28 days, the particles were completely covered by hydration products such as $CaSO_4 \cdot 2H_2O$ whiskers, $Ca(OH)_2$ crystals, C–S–H gel, and AFt crystals. The $CaSO_4 \cdot 2H_2O$ whiskers were continuously thickened and smoothed, and the needle-like AFt gradually increased, as shown in Figures 9(b) and 9(d). In addition, the large pores were filled with $CaSO_4 \cdot 2H_2O$ whiskers, C–S–H gel, AFt, and $Ca(OH)_2$ crystals. The bond between the hydration products and the particles became dense, but a large number of pores still existed compared with Figures 9(a) and 9(c). Consequently, this indicated that the hydration of HG in HPG had been basically completed, but the active SiO_2 and Al_2O_3 in PS were still slowly released and the hydration continued.

The above results indicated that the gelation essence of HPG-PS resulted from the hydration of HG in the HPG and active SiO_2 and Al_2O_3 in the PS, and the hydration of HG was significantly faster than that of PS. The hydration of HPG was dominated at the early curing stage, whereas the hydration of active SiO_2 and Al_2O_3 in PS mainly occurred in the late curing stages.

3.7.2. Effect of Soluble P and F on the Hydration of HPG-PS. The soluble P and F had significant effects on the hydration of HPG and PS [44]. The soluble P and F in the HPG and PS dissolved quickly in water and reacted with the $Ca(OH)_2$, as shown in equations (2) and (3); then, insoluble substances such as $Ca(PO_4)_2$ and CaF_2 were formed. These substances, adhering to the surfaces of the HPG and PS particles, increased the water impermeability of the formed alkaline membrane on the surface of the particles and retarded the hydration of HPG and PS. In addition, partial $Ca_3(PO_4)_2$ and CaF_2 gradually covered the surface of the particles and formed $Ca_{10}(PO_4)_6(OH)_2$ (hydroxyapatite), which further reduced the permeability of the semipermeable membrane [45]. Therefore, the continuous release process of active substances in PS, HPG, and cement was suppressed.

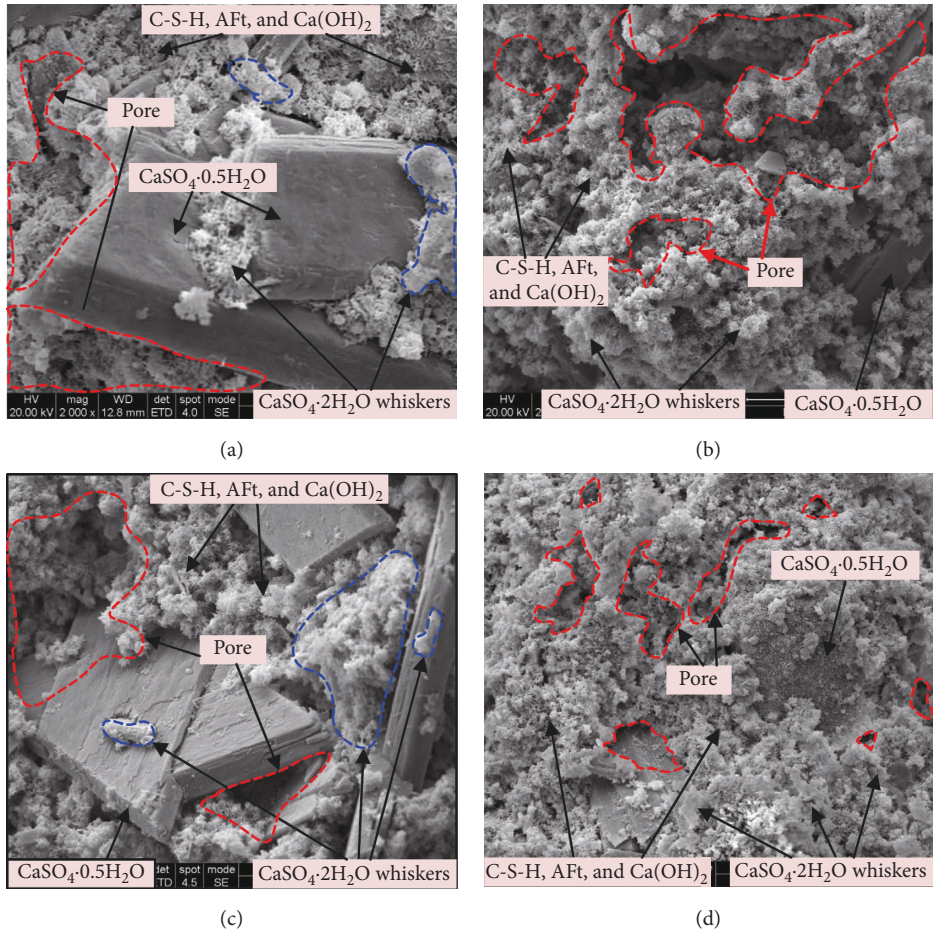

Figure 9: SEM images of specimens of backfill body. (a) S22 cured for 7 days; (b) S22 cured for 28 days; (c) S23 cured for 7 days; (d) S23 cured for 28 days.

When the soluble P and F were completely converted, the hydration process was gradually restored; so, it did not have a significant effect on the hydration in the later curing stage.

4. Application Evaluation

A phosphate mine in Guizhou province, China, adopted an upward horizontal slicing filling method with a production capacity of 700,000 t/a and a filling capacity of 100 m^3/h. HPG and PS are the main by-products of phosphoric acid and yellow phosphorus productions around this mine, with a wide range of sources, no payment, and short transport distances. Based on the recommended parameters, the amount of cement is greatly reduced in the CPB. The total cost of the backfill materials is 3.32 USD/m^3, which is only 29%–41% of CPB-based DPG-cement [26, 27] and 56% of CPB-based total tailings [35]. If an effective filling rate of 90% is taken into account as a rough calculation, then there will be a consumption of 300,000 tonnes of HPG and 50,000 tonnes of PS for CPB per year.

The engineering application proves that CPB-based HPG-PS is feasible and can be used in mines with similar situations. This technology has the advantages of simple preparation process, low cost, safety, and environment-friendly and can greatly increase the recovery of phosphate resources and the recycling of HPG and PS.

5. Conclusions

In this study, we investigated the application characteristics of recycling HPG and PS as cemented backfill materials in CPB under the modification of quicklime and cement by fluidity tests, gas detection, UCS tests, and scanning electron microscopy (SEM). On the basis of the results and discussion, the following conclusions were summarized:

(1) The addition of quicklime with 3% of HPG can eliminate CO_2, H_2S, and SO_2 generated in the pulping of CPB. The slump value decreases with the increase of HPG content and mass fraction. The slump values range between 15 mm and 35 mm when the HPG/PS ratios reach 6–10, which can meet the requirements for pipeline transportation of the paste.

(2) The UCS increases as HPG content and mass fraction increase. The losses in strength of CPB cured for 60–180 days are up to 18.08%–35.78% with the addition of 3% quicklime. The strength of CPB can maintain stability for a long time period while

adding 3% quicklime and 5% cement. The UCS of recommended specimens cured for 7 and 28 days is 1.15–2.10 MPa and 2.35–3.32 MPa, respectively, and the combined materials' cost is only 3.32 USD/m^3.

(3) The strength of CPB is the resultant of the combined hydration of HPG and PS. The soluble P and F delay the hydration of HPG and cement at the early curing stage, but having insignificant effect on the hydration of PS at the later curing stage.

(4) The pollutant indexes of the leachates meet Category IV of DZ/T 0290-2015. The HPG-PS materials have a certain consolidation action on P, F, and heavy metals, whereas the curing mechanism of the HPG-PS gelling system on P, F, and heavy metals needs to be further studied in the next work.

Data Availability

All data included in this study are available upon request by contacting the corresponding author.

Conflicts of Interest

The authors declare that they have no conflicts of interest.

Acknowledgments

The authors would like to thank the State Key Laboratory Open Foundation for Metal Mine Safety and Health of China (2017-JSKSSYS-03) and Ph.D. Research Startup Foundation of University of South China (2016XQD30).

References

[1] D. Nizevičienė, D. Vaičiukynienė, V. Vaitkevičius, and Ž. Rudžionis, "Effects of waste fluid catalytic cracking on the properties of semi-hydrate phosphogypsum," *Journal of Cleaner Production*, vol. 137, pp. 150–156, 2016.

[2] R. Pérez-López, F. Macías, C. R. Cánovas, A. M. Sarmiento, and S. M. Pérez-Moreno, "Pollutant flows from a phosphogypsum disposal area to an estuarine environment: an insight from geochemical signatures," *Science of the Total Environment*, vol. 553, pp. 42–51, 2016.

[3] G. Jiang, A. Wu, Y. Wang, and W. Lan, "Low cost and high efficiency utilization of hemihydrate phosphogypsum: used as binder to prepare filling material," *Construction and Building Materials*, vol. 167, pp. 263–270, 2018.

[4] H. Maghsoodloorad and A. Allahverdi, "Developing low-cost activators for alkali-activated phosphorus slag-based binders," *Journal of Materials in Civil Engineering*, vol. 29, no. 6, article 04017006, 2017.

[5] H. Mehdizadeh, E. Najafi Kani, A. Palomo Sanchez, and A. Fernandez-Jimenez, "Rheology of activated phosphorus slag with lime and alkaline salts," *Cement and Concrete Research*, vol. 113, pp. 121–129, 2018.

[6] M. Chen and T. E. Graedel, "A half-century of global phosphorus flows, stocks, production, consumption, recycling, and environmental impacts," *Global Environmental Change*, vol. 36, pp. 139–152, 2016.

[7] A. M. Rashad, "Phosphogypsum as a construction material," *Journal of Cleaner Production*, vol. 166, pp. 732–743, 2017.

[8] G. Ren, X. Yang, X. Wang, Z. Zhang, L. Yang, and B. Zhong, "Resource utilization of solid-phase by-product sulfate from industry production," *Phosphate & Compound Fertilizer*, vol. 33, pp. 32–36, 2018, in Chinese.

[9] Y. Tang, S. Hu, and W. Wang, "Study on leaching characteristics of phosphate from phosphorus slag," *Environmental Science & Technology*, vol. 38, pp. 383–385, 2015, in Chinese.

[10] T. Tian, Y. Yan, Z. Hu, Y. Xu, Y. Chen, and J. Shi, "Utilization of original phosphogypsum for the preparation of foam concrete," *Construction and Building Materials*, vol. 115, pp. 143–152, 2016.

[11] C. Sun, F. W. Zheng, Y. Y. Ren, G. B. Li, and Y. Su, "Research on utilization of yellow phosphorus slag," *Modern Chemical Industry*, vol. 37, pp. 28–31, 2017.

[12] A. Allahverdi and M. Mahinroosta, "Mechanical activation of chemically activated high phosphorous slag content cement," *Powder Technology*, vol. 245, pp. 182–188, 2013.

[13] Y. Shen, J. Qian, Y. Huang, and D. Yang, "Synthesis of belite sulfoaluminate-ternesite cements with phosphogypsum," *Cement and Concrete Composites*, vol. 63, pp. 67–75, 2015.

[14] R. K. Dutta, "Suitability of of flyash-lime-phosphogypsum composite in road pavements," *Periodica Polytechnica Civil Engineering*, vol. 60, pp. 455–469, 2016.

[15] O. Kumar, N. Abrantes, A. L. Caetano et al., "Phosphogypsum as a soil fertilizer: ecotoxicity of amended soil and elutriates to bacteria, invertebrates, algae and plants," *Journal of Hazardous Materials*, vol. 294, pp. 80–89, 2015.

[16] F. Yang, G. Li, H. Shi, and Y. Wang, "Effects of phosphogypsum and superphosphate on compost maturity and gaseous emissions during kitchen waste composting," *Waste Management*, vol. 36, pp. 70–76, 2015.

[17] J. Zhang and Y. Cao, "Study on leachate treatment for old phosphorous slag," *Desalination and Water Treatment*, vol. 44, no. 1–3, pp. 75–82, 2012.

[18] R. Pérez-López, J. M. Nieto, J. D. de la Rosa, and J. P. Bolívar, "Environmental tracers for elucidating the weathering process in a phosphogypsum disposal site: implications for restoration," *Journal of Hydrology*, vol. 529, pp. 1313–1323, 2015.

[19] L. Dong, D. Sun, X. Li, Z. Zhou, F. Gong, and X. Liu, "Theoretical and case studies of interval nonprobabilistic reliability for tailing dam stability," *Geofluids*, vol. 2017, Article ID 8745894, 11 pages, 2017.

[20] A. Wu, Y. Wang, H. Wang, S. Yin, and X. Miao, "Coupled effects of cement type and water quality on the properties of cemented paste backfill," *International Journal of Mineral Processing*, vol. 143, pp. 65–71, 2015.

[21] C. Qi, A. Fourie, and Q. Chen, "Neural network and particle swarm optimization for predicting the unconfined compressive strength of cemented paste backfill," *Construction and Building Materials*, vol. 159, pp. 473–478, 2018.

[22] E. Yilmaz and M. Fall, *Paste Tailings Management*, Springer International Publishing, Cham, Switzerland, 2017.

[23] S. Cao, W. Song, and E. Yilmaz, "Influence of structural factors on uniaxial compressive strength of cemented tailings backfill," *Construction and Building Materials*, vol. 174, pp. 190–201, 2018.

[24] L. Liu, Z. Fang, C. Qi, B. Zhang, L. Guo, and K.-I. Song, "Experimental investigation on the relationship between pore characteristics and unconfined compressive strength of cemented paste backfill," *Construction and Building Materials*, vol. 179, pp. 254–264, 2018.

[25] X. Li, Z. Zhou, G. Zhao, and Z. Liu, "Utilization of phosphogypsum for backfilling, way to relieve its environmental impact," *Gospodarka Surowcami Mineralnymi*, vol. 24, 2008.
[26] X.-m. Wang, B. Zhao, and Q.-l. Zhang, "Cemented backfill technology based on phosphorous gypsum," *Journal of Central South University of Technology*, vol. 16, no. 2, pp. 285–291, 2009.
[27] J.-s. Chen, B. Zhao, X.-m. Wang, Q.-l. Zhang, and L. Wang, "Cemented backfilling performance of yellow phosphorus slag," *International Journal of Minerals, Metallurgy, and Materials*, vol. 17, no. 1, pp. 121–126, 2010.
[28] F. Liu, "Application of phosphogypsum-based material to tailings backfill of phosphorite mine," *Journal of the Chemical Industry and Engineering Society of China*, vol. 60, pp. 3171–3177, 2009, in Chinese.
[29] W.-G. Dang, Z.-X. Liu, X.-Q. He, and Q.-L. Liu, "Mixture ratio of phosphogypsum in backfilling," *Mining Technology*, vol. 122, pp. 1–7, 2013.
[30] X. Li, J. Du, L. Gao et al., "Immobilization of phosphogypsum for cemented paste backfill and its environmental effect," *Journal of Cleaner Production*, vol. 156, pp. 137–146, 2017.
[31] Q. Chen, Q. Zhang, C. Qi, A. Fourie, and C. Xiao, "Recycling phosphogypsum and construction demolition waste for cemented paste backfill and its environmental impact," *Journal of Cleaner Production*, vol. 186, pp. 418–429, 2018.
[32] Q. Chen, Q. Zhang, A. Fourie, and C. Xin, "Utilization of phosphogypsum and phosphate tailings for cemented paste backfill," *Journal of Environmental Management*, vol. 201, pp. 19–27, 2017.
[33] Z. Duan, J. Li, T. Li et al., "Influence of crystal modifier on the preparation of α-hemihydrate gypsum from phosphogypsum," *Construction and Building Materials*, vol. 133, pp. 323–329, 2017.
[34] A. M. Rashad, "Potential use of phosphogypsum in alkali-activated fly ash under the effects of elevated temperatures and thermal shock cycles," *Journal of Cleaner Production*, vol. 87, pp. 717–725, 2015.
[35] Y. Zhou, H. Deng, and J. Liu, "Rational utilization of fine unclassified tailings and activated blast furnace slag with high calcium," *Minerals*, vol. 7, p. 48, 2017.
[36] L. Liu, Z. Y. Fang, Y. P. Wu, X. P. Lai, P. Wang, and K.-I. Song, "Experimental investigation of solid-liquid two-phase flow in cemented rock-tailings backfill using Electrical Resistance Tomography," *Construction and Building Materials*, vol. 175, pp. 267–276, 2018.
[37] N. Roussel, C. Stefani, and R. Leroy, "From mini-cone test to Abrams cone test: measurement of cement-based materials yield stress using slump tests," *Cement and Concrete Research*, vol. 35, pp. 817–822, 2005.
[38] H. Shen, A. Wu, L. Jiang, Y. Wang, H. Jiao, and X. Liu, "Small cylindrical slump test for unclassified tailings paste," *Journal of Central South University*, vol. 47, pp. 0204–0209, 2016, in Chinese.
[39] E. Yilmaz, T. Belem, M. Benzaazoua, and R. Ney, "Study of physico-chemical and mechanical characteristics of consolidated and unconsolidated cemented paste backfills," *Gospodarka Surowcami Mineralnymi-Mineral Resources Management*, vol. 29, pp. 81–100, 2013.
[40] A. Kesimal, E. Yilmaz, B. Ercikdi, I. Alp, and H. Deveci, "Effect of properties of tailings and binder on the short-and long-term strength and stability of cemented paste backfill," *Materials Letters*, vol. 59, no. 28, pp. 3703–3709, 2005.
[41] B. Zhang, W. Zhou, H. Zhao, Z. Tian, F. Li, and Y. Wu, "Stabilization/solidification of lead in MSWI fly ash with mercapto functionalized dendrimer Chelator," *Waste Management*, vol. 50, pp. 105–112, 2016.
[42] S. Li, Y. Ai, L. Liu, and X. Huang, "Research on mechanical properties and softening coefficient of hemihydrate-slag cement," *Bulletin of the Chinese Ceramic Society*, vol. 30, pp. 732–735, 2011, in Chinese.
[43] L. Svatovskaya, M. Shershneva, M. Baydarashvily, A. Sychova, M. Sychov, and M. Gravit, "Geoecoprotective properties of cement and concrete against heavy metal ions," *Procedia Engineering*, vol. 117, pp. 345–349, 2015.
[44] C. Guo, J. Zhu, W. Zhou, Z. Sun, and W. Chen, "Effect of phosphorus and fluorine on hydration process of tricalcium silicate and tricalcium aluminate," *Journal of Wuhan University of Technology*, vol. 27, pp. 333–336, 2012, in Chinese.
[45] K. Kiminami, K. Matsuoka, T. Konishi et al., "Effects of addition of α-tricalcium phosphate powders on material properties of the chelate-setting hydroxyapatite cement," *Phosphorus Research Bulletin*, vol. 33, pp. 7–13, 2017.